Voltage-Controlled Antiferromagnetism in Magnetic Tunnel Junctions

Meng Xu,[1] Mingen Li,[2] Pravin Khanal,[1] Ali Habiboglu,[1] Blake Insana,[1] Yuzan Xiong,[3,4] Thomas Peterson,[5] Jason C. Myers,[6] Deborah Ortega,[1] Hongwei Qu,[4] C. L. Chien,[2] Wei Zhang,[3] Jian-Ping Wang,[5] and W. G. Wang[1,*]

[1]*Department of Physics, University of Arizona, Tucson, Arizona 85721, USA*
[2]*Department of Physics and Astronomy, The Johns Hopkins University, Baltimore, Maryland 21218, USA*
[3]*Department of Physics, Oakland University, Rochester, Michigan 48309, USA*
[4]*Department of Electrical and Computer Engineering, Oakland University, Rochester, Michigan 48309, USA*
[5]*Department of Electrical and Computer Engineering, University of Minnesota, 200 Union Street Southeast, Minneapolis, Minnesota 55455, USA*
[6]*Characterization Facility, University of Minnesota, 100 Union Street Southeast, Minneapolis, Minnesota 55455, USA*

(Received 20 December 2019; revised manuscript received 12 March 2020; accepted 2 April 2020; published 7 May 2020)

We demonstrate a voltage-controlled exchange bias effect in CoFeB/MgO/CoFeB magnetic tunnel junctions that is related to the interfacial $Fe(Co)O_x$ formed between the CoFeB electrodes and the MgO barrier. The unique combination of interfacial antiferromagnetism, giant tunneling magnetoresistance, and sharp switching of the perpendicularly magnetized CoFeB allows sensitive detection of the exchange bias. We find that the exchange bias field can be isothermally controlled by magnetic fields at low temperatures. More importantly, the exchange bias can also be effectively manipulated by the electric field applied to the MgO barrier due to the voltage-controlled antiferromagnetic anisotropy in this system.

DOI: 10.1103/PhysRevLett.124.187701

Recent research on the interaction between electric fields and magnetic order has yielded some very interesting results [1–4]. In ferromagnetic systems with 3*d* transitional metals, it was shown that electric fields can effectively change the perpendicular magnetic anisotropy (PMA) [5–7], leading to low-energy switching of magnetization on the subnanosecond timescale [8,9]. Electric field driven ionic migration can also have a large impact on the saturation magnetization of the 3*d* ferromagnets (FMs), resulting in a giant modulation of magnetism [10–12]. On the other hand, antiferromagnets (AFMs) possess several unique features, such as staggered arrangement of spins, resilience to external magnetic fields, and much higher resonance frequency in the terahertz range [13–15]. Electrical control of magnetism in antiferromagnetic (AF) systems has also attracted a great deal of attention. A pioneering example can be found in Cr_2O_3 [16]. The AF order parameter of the magnetoelectric Cr_2O_3 can be reversibly and deterministically switched by voltages, manifested by the exchange bias effect experienced by the adjacent FM layer [17–19], similar to those observed in multiferroic systems [20,21]. Other examples include noncentrosymmetric antiferromagnets, such as CuMnAs [22] and Mn_2Au [23], where the AF order parameter may be switched by electrical currents. The AF order can also be electrically controlled by adjusting the exchange spring [24], by spin-orbit torques [25], and through coupling with a ferroelectric substrate, as recently demonstrated [26].

In this Letter, we report the discovery of the voltage-controlled antiferromagnetism in a model spintronics system that is also technologically important: the CoFeB/MgO/CoFeB perpendicular magnetic tunnel junction (p-MTJ). It is demonstrated for the first time through transport measurement that at low temperature the CoFeB layers are exchange biased to the interfacial $Fe(Co)O_x$ layers naturally formed between CoFeB and the MgO barrier. In addition to the voltage-controlled magnetic anisotropy (VCMA) effect [5–7], the electric field can have a profound impact on the exchange bias field (H_{EB}) in this system. Thanks to the giant tunneling magnetoresistance (TMR) and the sharp switching of the CoFeB layers with PMA, a clear dependence of H_{EB} on the applied voltage has been detected, which is attributed to the voltage control of AF anisotropy.

The MTJ thin films are fabricated using magnetron sputtering with the core structure $Co_{20}Fe_{60}B_{20}(0.8\ \text{nm})/MgO(1-3.5\ \text{nm})/Co_{20}Fe_{60}B_{20}(1.6\ \text{nm})$. More information on the MTJ fabrication can be found in the Supplemental Material [27], which includes Refs. [28–41]. After annealed at 300 °C for 10 min, the TMR curve of a junction was measured under perpendicular field at room temperature (RT) as shown in Fig. 1(a). The barrier thickness is 3 nm and the resistance area product is $5 \times 10^7\ \Omega\,\mu\text{m}^2$. The black curve exhibits sharp switches with a TMR value of 120%, a ratio that is typical for MTJs annealed at this condition [30]. Then the sample is cooled under a perpendicular field of +3000 Oe. The resistance of the antiparallel state (R_{AP}) consistently increases with decreasing temperature, while the resistance of the parallel state (R_P) remains largely unchanged, leading to a TMR value that is

 © 2020 American Physical Society

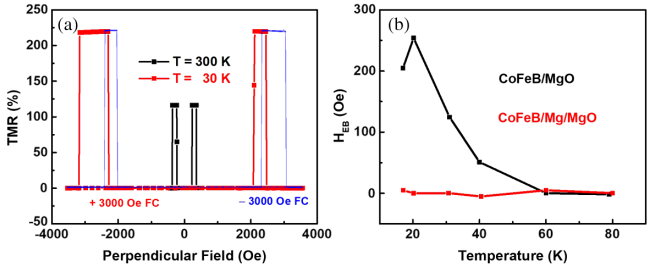

FIG. 1. (a) TMR curves of a p-MTJ measured at RT (black) and 30 K (red and light blue). While no exchange bias is observed at RT, after cooling down to 30 K under a perpendicular field of ±3000 Oe, obvious H_{EB} for the soft and hard FM layers can be observed. (b) Temperature dependence of H_{EB} measured for two samples in the Hall bar geometry, showing the observed exchange bias originates from the FM/MgO interface.

almost doubled compared with that at RT (see Supplemental Material [27], Fig. S1). Unlike the TMR curve measured at RT, where the switching fields of the soft (bottom, 0.8 nm) and hard (top, 1.6 nm) CoFeB layers are symmetric about zero field, the switching fields at 30 K are shifted negatively. Reversing the cooling field to −3000 Oe changes the switching fields to the positive direction, as shown by the light blue curve. This is direct evidence of the exchange bias effect in the system. Here we define the exchange bias field H_{EB} as $(H_{C1} + H_{C2})/2$, where H_{C1} (H_{C2}) is the negative (positive) switching field of a given FM layer. The magnitude of H_{EB} is about 100 Oe for the soft layer (SL) and 350 Oe for the hard layer (HL) with both polarities opposite to the cooling field.

To the best of our knowledge, this is the first observation of exchange bias via the TMR measurement in a p-MTJ with no active AF layers, such as IrMn or PtMn. Previously, the interfacial spins of a thick Fe layer (10 nm) adjacent to MgO were demonstrated to be exchange biased using the magnetization-induced second harmonic generation (MSHG) technique [42], and the existence of exchange bias was indirectly inferred by the ferromagnetic resonance (FMR) measurement [43]. Here, due to the reduced thickness of the FM layers (∼1 nm), the entire magnetization, instead of only the interfacial spins [42], is exchange biased. With the sharp switching of perpendicularly magnetized CoFeB, now the exchange bias effect can be sensitively detected by the TMR measurement. It is known that oxygen ions generated during rf sputtering can bombard and oxidize adjacent Fe(Co) to form FeO_x and CoO_x at the bottom CoFeB/MgO interface, while thermally induced oxidation or reduction could also take place during the postgrowth annealing [41]. Therefore, the exchange bias effect is most likely linked to the antiferromagnetism associated with the Fe (Co)—O bonding. To verify this assumption, two Hall bars resembling the bottom FM layer of the p-MTJs are fabricated, one with the structure of Ta/CoFeB(0.8 nm)/MgO(3 nm)/Ta and the other with the structure of Ta/CoFeB(0.8 nm)/Mg(0.6 nm)/MgO(3 nm)/Ta. It is expected that the Fe (Co)—O bonding in the latter is greatly weakened due to the Mg insertion. As illustrated by the temperature dependence of H_{EB} in Fig. 1(b), the exchange field in the sample with Mg insertion is dramatically reduced, thus unambiguously demonstrating that the exchange bias effect observed in Fig. 1(a) is caused by the antiferromagnetism associated with Fe (Co)—O bonding. The p-MTJs in this study are of high quality, as demonstrated by the large TMR ratio close to 400% at low temperature (Supplemental Material [27]), indicating no severe oxidation of the CoFeB layers. Therefore the FeO_x or CoO_x formed between CoFeB and MgO is likely to be only a monolayer or submonolayer, which is consistent with the sub-100 K blocking temperature (T_B) observed.

To this point, the exchange bias effect in our sample behaves similar to those in a typical FM-AFM bilayer system [44]. Generally speaking, the exchange bias field is only observed when the FM is cooled below T_N under an external magnetic field. After the H_{EB} has been set, its polarity cannot be changed solely by reversing the magnetic field without warming above T_N. In rare cases, isothermal switching of H_{EB} could happen under spin-flop transition, but with very high switching fields (over 10 T) [45]. In sharp contrast, isothermal switching of H_{EB} can be achieved in our system with a relatively small magnetic field, as demonstrated in Fig. 2(a). First, the p-MTJ was cooled from RT to 30 K under a positive magnetic field, thereby setting a negative H_{EB} for both FM layers. Then a setting field of −4500 Oe was applied isothermally, followed by the subsequent measurement of the TMR curve. Interestingly, positive H_{EB} values of +100 and +350 Oe were obtained for the two FM layers. The same procedure was performed with a +4500 Oe setting field and the H_{EB} switched to −100 and −350 Oe. The relatively small setting field of ±4500 Oe indicates the antiferromagnetism at the FM-oxide interface is weak, which is consistent with the very thin $Fe(Co)O_x$ formed between the CoFeB and MgO. Notably, the H_{EB} can be reversibly and deterministically controlled by the setting field as shown in the inset

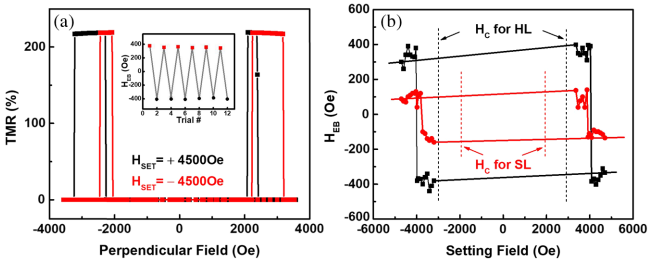

FIG. 2. (a) Representative TMR curves taken after the application of −4500 Oe setting field (red) and after the application of +4500 Oe setting field (black). (Inset) Reversible and deterministic control of H_{EB} by applying setting field isothermally. (b) H_{EB} dependence on external setting field for both FM layers. Dashed lines indicated their respective coercivities. All data are collected at the constant temperature of 30 K.

of Fig. 2(a), demonstrating the robustness of this effect. Here we define the minimum field that switches H_{EB} isothermally as H_{AF}. To determine H_{AF}, the sample was first initialized with a large positive (negative) field (>6000 Oe), which set the H_{EB} to be negative (positive). Then the TMR curves were measured after incremental setting field applied and the corresponding H_{EB} values are plotted in Fig. 2(b). Two features immediately emerge in the setting field dependence of H_{EB}. First, H_{AF} is symmetric about the zero setting field. Second, H_{AF} is different for soft and hard layers, which further confirms the interfacial origin of the exchange bias. Note the exchange bias can only be observed when the maximum magnetic field applied during TMR measurement is smaller than H_{AF}. Otherwise, the exchange bias will simply manifest itself as coercivity enhancement and there will be no shift in the TMR curve.

The exchange bias effect can be usually understood through the schematic diagram shown in Fig. 3(a) [44]. The bottom FM spins are coupled to the uncompensated interfacial spins (blue arrows) that are strongly pinned by the AFM (black arrows). Since the AFM is insensitive to the external field, FM spins are biased to one specific direction determined by the direction of uncompensated spins and the nature of exchange coupling (FM or AF). Within this context, the exchange bias effect in our sample can be schematically represented by a simplified model shown in Fig. 3(b). The interfacial Fe(Co)O_x layer serves as the AF layer (black arrows) between CoFeB and MgO. The circled spins are uncompensated and moderately pinned by the surrounding AF spins. For simplicity, the AF spins are shown to form one monolayer. In reality, they may form discrete patches that are more or less randomly distributed at the interface [42], as indicated by the spin-glass-like feature shown in Fig. S2 of the Supplemental Material [27]. The isothermal control of H_{EB} by the magnetic field stems from the weak AF order of the interfacial Fe(Co)O_x. When the external field exceeds H_{C2} but below H_{AF}, the circled (pinned) spins and the surrounding AF spins remain unchanged, leading to an H_{EB} observed in the hysteresis loop. When the external setting field exceeds H_{AF}, the pinned spins would be reversed to lower the Zeeman energy, which simultaneously rotates the AF spins. Subsequent TMR measurement would produce an H_{EB} with the opposite sign. This picture qualitatively describes the isothermal switching of H_{EB} presented in Fig. 2. H_{EB} appears when $H_C < H_{AF}$ and the applied magnetic field is smaller than H_{AF}.

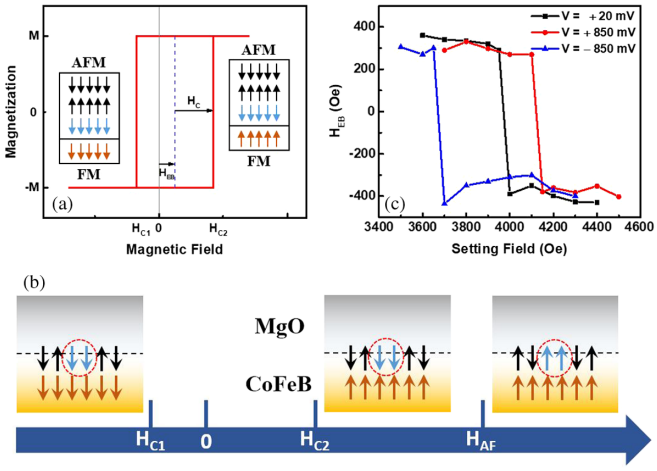

FIG. 3. (a) Schematic picture of the exchange bias effect in AFM-FM bilayers, where the exchange coupling between the FM spins (brown) and the uncompensated interfacial spins (blue) of the AFM (black) leads to a shift of the hysteresis loop characterized by H_{EB}. (b) Schematic diagram of the isothermal control of H_{EB} with magnetic field. H_{C1} and H_{C2} are the magnetization switching fields in negative and positive field direction. H_{AF} is the critical setting field above which H_{EB} polarity changes. (c) Setting field dependence of the hard layer H_{EB} in a p-MTJ under different voltages, in which the positive voltage increases H_{AF} and the negative voltage reduces H_{AF}.

One important feature of the CoFeB-MgO p-MTJ is the interfacial PMA and the associated VCMA effect. The PMA is the result of the hybridization of 3d orbitals of Fe and 2p orbitals of oxygen [46]. When an electric field is applied to the junction, it modifies the electron occupation in different orbitals through the Fe—O bonding, thus leading to a change of magnetic anisotropy energy [47]. Since the presence of exchange bias and isothermal control of H_{EB} by the magnetic field is also caused by Fe(Co)—O bonding at the interface, one may anticipate a correlation between the exchange bias and the electric field in the system. To test this point, an experiment similar to the one in Fig. 2(b) was performed, only this time with voltage applied to the junction when the setting magnetic field is turned on. Note the H_{EB} is still measured by the TMR curve under low bias voltage (~10 mV) after the removal of the setting field and voltage. Remarkably, a clear dependence of H_{AF} on the applied voltage now appears. As shown in Fig. 3(c), H_{AF} can be effectively increased (reduced) by positive (negative) voltages. The applied voltage of ±850 mV can cause a total modification of 400 Oe in H_{AF}. Note only the positive branch of the hard layer H_{EB} is plotted in Fig. 3(c) to highlight the changes brought on by voltage.

If the voltage can modulate H_{AF}, one may expect the associated change of antiferromagnetism to be reflected by the TMR curve as well. The magnetoresistance of the p-MTJ was measured at different voltages and plotted in Fig. 4(a). Indeed, very different TMR curves are obtained. It is known that the H_C of the two FM layers can be altered by the VCMA effect, which gives rise to very distinct TMR curves under different voltages [7]. The p-MTJs in this study do exhibit the conventional VCMA effect, as evidenced by the voltage dependence of the switching fields for the hard layer at RT [Fig. 4(b)], where modulation of coercivity is centered around the zero field. The behavior

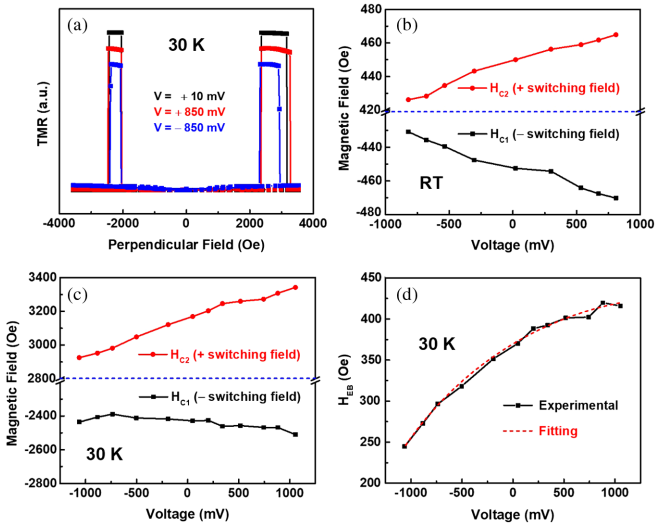

FIG. 4. (a) Representative TMR curves measured under different bias voltages at 30 K. (b) The voltage dependence of magnetization switching fields H_{C1} and H_{C2} at RT, as a result of the VCMA effect. (c) The voltage dependence of H_{C1} and H_{C2} at 30 K, as a result of both the VCMA and voltage-controlled exchange bias effects. (d) Voltage dependence of the exchange bias field at 30 K. Experimental data are fitted using Eq. (1) assuming a linear voltage dependence for K_{AF}.

of TMR curves in Fig. 4(a), however, are markedly different from those influenced only by the VCMA effect. Here the pronounced changes are observed under *positive* magnetic field only. A closer inspection reveals that now the changes of H_{C1} and H_{C2} are asymmetric about the zero magnetic field, as shown in Fig. 4(c). This sample was initialized with a large negative field, resulting in a positive H_{EB}. As positive voltage leads to a stronger interaction between the pinned uncompensated spins and the surrounding AF regions [Fig. 3(c)], and the FM magnetization becomes harder to switch up (leading to a larger H_{C2}) and easier to switch down (leading a smaller H_{C1}). Under negative magnetic field, this phenomenon counteracts with the VCMA effect that enhances H_{C1}, leading to a weaker dependence of H_{C1} on voltage. Simultaneously, a stronger voltage dependence of H_{C2} emerges as these two effects facilitate each other under positive magnetic field. A direct result of this asymmetric dependence of the switching fields on voltage is the shift of the hysteresis loop by voltage, namely, the voltage-controlled exchange bias effect. The voltage dependence of H_{EB} is plotted in Fig. 4(d). A monotonic (but nonlinear) dependence of H_{EB} on voltage can be seen, where the exchange bias is enhanced by positive voltage and reduced by negative voltage. The modification of H_{EB} is quite significant, with a change of more than 150 Oe observed when the voltage is varied between +1 and −1 V.

We attempt to understand the voltage dependence of H_{EB} through the model developed by Malozemoff, considering the random field at the interface [48]

$$H_{EB} = \frac{2f_i}{\pi^2}\sqrt{A_{AF}K_{AF}}/M_{FM}t_{FM}, \quad (1)$$

where f_i is of order unity and determined by the microscopic interfacial conditions, A_{AF} and K_{AF} are the exchange stiffness and anisotropy of AFM. H_{EB} calculated using this equation is of the same order as experimental observation for typical FM-AFM systems. In Eq. (1), H_{EB} depends explicitly on A_{AF}, K_{AF}, and M_{FM} for a given FM with a fixed thickness. Generally, the dependence of M_{FM} on voltage is negligibly small without the ionic effect [10–12]. A_{AF} can, in principle, be modified by voltage, but this effect is not considered here because the change of stiffness is also much smaller compared to that of anisotropy, as demonstrated in the FM case [49]. The results in Fig. 4(d) then indicate the change of H_{EB} is due to the control of K_{AF} by voltage. If we assume the AFM anisotropy to be linearly dependent on voltage as $K_{AF} = K_0 + \xi * V$, the data indeed can be well fitted by Eq. (1) as shown by the red curve in Fig. 4(d). The increase in H_{EB} at +1 V (+330 mV/nm) corresponds to a 36% increase in K_{AF} compared with the zero-bias value. This behavior of H_{EB} can be well captured by the square root dependence of K_{AF} that is linearly modulated by voltage, which clearly demonstrates the voltage-controlled antiferromagnetism effect in the CoFeB-MgO p-MTJs.

Using an empirical A_{AF} value (10^{-12}–10^{-13} J/m^3) [50], we obtain the effective $K_{AF} \sim 10^4$ J/m^3, which is about 2 orders of magnitude smaller than K_{AF} of thick AFM layers [51]. From the fitting result of ξ in Fig. 4(d), we can extract the linear coefficient of voltage-controlled AF anisotropy to be 22 fJ/V m [assuming an A_{AF} of 5×10^{-13} J/m and Fe(Co)O_x monolayer thickness of 4.3 Å], which represents the scale of voltage-controlled AF effect in this system. The physical origin of the voltage control of K_{AF} is likely related to the electrically induced orbital reconstruction [52]. However, a more quantitative understanding requires further theoretical and experimental investigation, which is beyond the scope of the current Letter. Here we provide a simplified picture to understand the results in Fig. 4: for pinned uncompensated spins below T_B, their stability is determined by the interactions with the FM and AF portion of the system. Voltage application may modulate both interactions via voltage-controlled FM and AF anisotropy. In this study, the applied field and the unidirectional magnetic anisotropy (defined as $H_{EB} \times M_{FM} \times t_{FM}$) direction are collinear. Therefore H_{EB} is independent of FM uniaxial anisotropy [53]. Voltage only significantly changes the exchange interaction between the pinned spins and the antiferromagnet by modulating the AF anisotropy, which effectively modifies the pinning site stability and leads to a change in H_{EB} following Malozemoff's model.

Finally, we would also like to comment on the implication of our results on the understanding of the magnetoresistance of CoFeB/MgO/CoFeB MTJs, where a large

TMR is always preferred. Our study provides an important clue to understand the discrepancy between the predicted (up to 35 000% [54,55]) and the observed (~400%–1000% [33,56,57]) TMR values in this system. Among many factors that could reduce the experimental TMR ratio, the interfacial oxidation plays an important role as one monolayer of oxide at the Fe/MgO interface can decrease the TMR by more than 10 times, as shown by a density functional theory calculation [58]. However, prior to our study, it is unknown if a very thin FeO/CoO layer could exist in high-quality p-MTJs without detrimentally destroying TMR. No actual TMR has been demonstrated in previous studies where the interfacial oxide was probed by MSHG [42] or FMR [43]. Here the observation of exchange bias in our high-quality p-MTJ and the transmission electron microscopy study at the CoFeB/MgO interface (Supplemental Material [27], Fig. S6) unambiguously demonstrate the existence of the FeO/CoO layers. Therefore the interfacial oxidation could be the main reason that limits the TMR in CoFeB/MgO/CoFeB MTJs.

To conclude, we have demonstrated that the exchange bias in the CoFeB/MgO/CoFeB p-MTJ with giant magnetoresistance can be effectively controlled by voltage. The square root dependence of the exchange bias field on voltage can be well explained by an AF anisotropy energy that is linearly modulated by voltage. Similar manipulation of exchange bias and antiferromagnetism may be realized in a wide range of other FM-oxide and FM-AFM systems. These results also provide insight into a better understanding of the complex CoFeB/MgO interface and represent a new route to manipulate p-MTJs by controlling exchange bias.

The authors would like to thank Shufeng Zhang and Yihong Cheng for inspiring discussion. This work was supported in part by DARPA through the ERI program (FRANC), by NSF through ECCS-1554011, and by Semiconductor Research through the Global Research Collaboration program. W. Z. acknowledges support from AFOSR under Grant No. FA9550-19-1-0254. T. P. acknowledges support from the NSF Scalable Parallelism in the Extreme (SPX) Grant. The TEM study was supported in part by NSF through the UMN MRSEC program.

*wgwang@physics.arizona.edu

[1] N. A. Spaldin and M. Fiebig, Science **309**, 391 (2005).
[2] M. Bibes and A. Barthélémy, Nat. Mater. **7**, 425 (2008).
[3] N. X. Sun and G. Srinivasan, Spin **02**, 1240004 (2012).
[4] F. Matsukura, Y. Tokura, and H. Ohno, Nat. Nanotechnol. **10**, 209 (2015).
[5] M. Weisheit, S. Fähler, A. Marty, Y. Souche, C. Poinsignon, and D. Givord, Science **315**, 349 (2007).
[6] T. Maruyama, Y. Shiota, T. Nozaki, K. Ohta, N. Toda, M. Mizuguchi, A. A. Tulapurkar, T. Shinjo, M. Shiraishi, S. Mizukami, Y. Ando, and Y. Suzuki, Nat. Nanotechnol. **4**, 158 (2009).
[7] W.-G. Wang, M. Li, S. Hageman, and C. L. Chien, Nat. Mater. **11**, 64 (2012).
[8] C. Grezes, F. Ebrahimi, J. G. Alzate, X. Cai, J. A. Katine, J. Langer, B. Ocker, P. Khalili, and K. L. Wang, Appl. Phys. Lett. **108**, 012403 (2016).
[9] S. Kanai, F. Matsukura, and H. Ohno, Appl. Phys. Lett. **108**, 192406 (2016).
[10] C. Bi, Y. Liu, T. Newhouse-Illige, M. Xu, M. Rosales, J. W. Freeland, O. Mryasov, S. Zhang, S. G. E. te Velthuis, and W. G. Wang, Phys. Rev. Lett. **113**, 267202 (2014).
[11] U. Bauer, L. Yao, A. Tan, P. Agrawal, S. Emori, H. L. Tuller, S. van Dijken, and G. S. D. Beach, Nat. Mater. **14**, 174 (2015).
[12] C. Leighton, Nat. Mater. **18**, 13 (2019).
[13] V. Baltz, A. Manchon, M. Tsoi, T. Moriyama, T. Ono, and Y. Tserkovnyak, Rev. Mod. Phys. **90**, 015005 (2018).
[14] T. Jungwirth, X. Marti, P. Wadley, and J. Wunderlich, Nat. Nanotechnol. **11**, 231 (2016).
[15] A. H. MacDonald and M. Tsoi, Phil. Trans. R. Soc. A **369**, 3098 (2011).
[16] P. Borisov, A. Hochstrat, X. Chen, W. Kleemann, and C. Binek, Phys. Rev. Lett. **94**, 117203 (2005).
[17] X. He, Y. Wang, N. Wu, A. N. Caruso, E. Vescovo, K. D. Belashchenko, P. A. Dowben, and C. Binek, Nat. Mater. **9**, 579 (2010).
[18] S. P. Pati, M. Al-Mahdawi, S. Ye, Y. Shiokawa, T. Nozaki, and M. Sahashi, Phys. Rev. B **94**, 224417 (2016).
[19] Y. Shiratsuchi, T. V. A. Nguyen, and R. Nakatani, J. Magn. Soc. Jpn. **42**, 119 (2018).
[20] S. M. Wu, S. A. Cybart, P. Yu, M. D. Rossell, J. X. Zhang, R. Ramesh, and R. C. Dynes, Nat. Mater. **9**, 756 (2010).
[21] Q. Yang, Z. Zhou, N. X. Sun, and M. Liu, Phys. Lett. A **381**, 1213 (2017).
[22] P. Wadley *et al.*, Science **351**, 587 (2016).
[23] S. Y. Bodnar, L. Šmejkal, I. Turek, T. Jungwirth, O. Gomonay, J. Sinova, A. A. Sapozhnik, H.-J. Elmers, M. Kläui, and M. Jourdan, Nat. Commun. **9**, 348 (2018).
[24] Y. Wang, X. Zhou, C. Song, Y. Yan, S. Zhou, G. Wang, C. Chen, F. Zeng, and F. Pan, Adv. Mater. **27**, 3196 (2015).
[25] P. H. Lin, B. Y. Yang, M. H. Tsai, P. C. Chen, K. F. Huang, H. H. Lin, and C. H. Lai, Nat. Mater. **18**, 335 (2019).
[26] X. Chen, X. Zhou, R. Cheng, C. Song, J. Zhang, Y. Wu, Y. Ba, H. Li, Y. Sun, Y. You, Y. Zhao, and F. Pan, Nat. Mater. **18**, 931 (2019).
[27] See Supplemental Material at http://link.aps.org/supplemental/10.1103/PhysRevLett.124.187701 for more details on the experiment and analysis, which includes Refs. [28–41].
[28] C. H. Shang, J. Nowak, R. Jansen, and J. S. Moodera, Phys. Rev. B **58**, R2917 (1998).
[29] L. Yuan, S. H. Liou, and D. Wang, Phys. Rev. B **73**, 134403 (2006).
[30] H. Almasi, D. R. Hickey, T. Newhouse-Illige, M. Xu, M. R. Rosales, S. Nahar, J. T. Held, K. A. Mkhoyan, and W. G. Wang, Appl. Phys. Lett. **106**, 182406 (2015).
[31] W. G. Wang, C. Ni, G. X. Miao, C. Weiland, L. R. Shah, X. Fan, P. Parson, J. Jordan-sweet, X. M. Kou, Y. P. Zhang, R. Stearrett, E. R. Nowak, R. Opila, J. S. Moodera, and J. Q. Xiao, Phys. Rev. B **81**, 144406 (2010).
[32] M. Finazzi, A. Brambilla, L. Duò, G. Ghiringhelli, M. Portalupi, F. Ciccacci, M. Zacchigna, and M. Zangrando, Phys. Rev. B **70**, 235420 (2004).

[33] H. Almasi, M. Xu, Y. Xu, T. Newhouse-Illige, and W. G. Wang, Appl. Phys. Lett. **109**, 032401 (2016).
[34] I. L. Guhr, O. Hellwig, C. Brombacher, and M. Albrecht, Phys. Rev. B **76**, 064434 (2007).
[35] J. Gurgul, E. Młyńczak, A. Kozioł-Rachwał, K. Matlak, K. Freindl, E. Madej, N. Spiridis, T. Ślęzak, and J. Korecki, Phys. Rev. B **96**, 104421 (2017).
[36] M. Ali, P. Adie, C. H. Marrows, D. Greig, B. J. Hickey, and R. L. Stamps, Nat. Mater. **6**, 70 (2007).
[37] W. Wang, F. Takano, M. Takenaka, H. Akinaga, and H. Ofuchi, J. Appl. Phys. **103**, 093914 (2008).
[38] W. Zhang, T. Wen, and K. M. Krishnan, Appl. Phys. Lett. **101**, 132401 (2012).
[39] O. Ozatay, P. G. Gowtham, K. W. Tan, J. C. Read, K. A. Mkhoyan, M. G. Thomas, G. D. Fuchs, P. M. Braganca, E. M. Ryan, K. V. Thadani, J. Silcox, D. C. Ralph, and R. A. Buhrman, Nat. Mater. **7**, 567 (2008).
[40] A. Picone, M. Riva, A. Brambilla, A. Calloni, G. Bussetti, M. Finazzi, F. Ciccacci, and L. Duò, Surf. Sci. Rep. **71**, 32 (2016).
[41] J. C. Read, P. G. Mather, and R. A. Buhrman, Appl. Phys. Lett. **90**, 132503 (2007).
[42] Y. Fan, K. J. Smith, G. Lüpke, A. T. Hanbicki, R. Goswami, C. H. Li, H. B. Zhao, and B. T. Jonker, Nat. Nanotechnol. **8**, 438 (2013).
[43] I. Barsukov, Y. Fu, A. M. Gonçalves, M. Spasova, M. Farle, L. C. Sampaio, R. E. Arias, and I. N. Krivorotov, Appl. Phys. Lett. **105**, 152403 (2014).
[44] J. Nogués and I. K. Schuller, J. Magn. Magn. Mater. **192**, 203 (1999).
[45] J. Nogués, J. Sort, S. Suriñach, J. S. Muñoz, M. D. Baró, J. F. Bobo, U. Lüders, E. Haanappel, M. R. Fitzsimmons, A. Hoffmann, and J. W. Cai, Appl. Phys. Lett. **82**, 3044 (2003).
[46] H. X. Yang, M. Chshiev, B. Dieny, J. H. Lee, A. Manchon, and K. H. Shin, Phys. Rev. B **84**, 054401 (2011).
[47] M. K. Niranjan, C. G. Duan, S. S. Jaswal, and E. Y. Tsymbal, Appl. Phys. Lett. **96**, 222504 (2010).
[48] A. P. Malozemoff, Phys. Rev. B **35**, 3679 (1987).
[49] J. Cho, S. Miwa, K. Yakushiji, H. Kubota, A. Fukushima, C. Y. You, S. Yuasa, and Y. Suzuki, Phys. Rev. Applied **10**, 014033 (2018).
[50] G. Fischer, M. Däne, A. Ernst, P. Bruno, M. Lüeders, Z. Szotek, W. Temmerman, and W. Hergert, Phys. Rev. B **80**, 014408 (2009).
[51] M. D. Rechtin and B. L. Averbach, Phys. Rev. B **6**, 4294 (1972).
[52] C. Song, B. Cui, F. Li, X. Zhou, and F. Pan, Prog. Mater. Sci. **87**, 33 (2017).
[53] A. Hoffmann, M. Grimsditch, J. E. Pearson, J. Nogués, W. A. A. Macedo, and I. K. Schuller, Phys. Rev. B **67**, 220406(R) (2003).
[54] W. H. Butler, Sci. Technol. Adv. Mater. **9**, 014106 (2008).
[55] W. H. Butler, X.-G. Zhang, T. C. Schulthess, and J. M. MacLaren, Phys. Rev. B **63**, 054416 (2001).
[56] S. Ikeda, J. Hayakawa, Y. Ashizawa, Y. M. Lee, K. Miura, H. Hasegawa, M. Tsunoda, F. Matsukura, and H. Ohno, Appl. Phys. Lett. **93**, 082508 (2008).
[57] D. Apalkov, B. Dieny, and J. M. Slaughter, Proc. IEEE **104**, 1796 (2016).
[58] X. G. Zhang and W. H. Butler, J. Phys. Condens. Matter **15**, R1603 (2003).